Developmental Cognitive Neuroscience 24 (2017) 118–128

Contents lists available at ScienceDirect

Developmental Cognitive Neuroscience

journal homepage: http://www.elsevier.com/locate/dcn

How does the body representation system develop in the human brain?

Aurelie Fontan[a,b], Fabien Cignetti[a,b], Bruno Nazarian[c], Jean-Luc Anton[c], Marianne Vaugoyeau[a,b], Christine Assaiante[a,b,*]

[a] Aix Marseille Univ, CNRS, LNC, Laboratoire de Neurosciences Cognitives, Marseille, France
[b] Aix Marseille Univ, CNRS, Fédération 3C, Marseille, France
[c] Aix-Marseille Université, CNRS, INT UMR 7289, Centre IRM, France

ARTICLE INFO

Article history:
Received 9 September 2016
Received in revised form
27 December 2016
Accepted 25 February 2017
Available online 28 February 2017

Keywords:
Body representation system
Proprioception
fMRI
DTI
VBM
Children

ABSTRACT

Exploration of the body representation system (BRS) from kinaesthetic illusions in fMRI has revealed a complex network composed of sensorimotor and frontoparietal components. Here, we evaluated the degree of maturity of this network in children aged 7–11 years, and the extent to which structural factors account for network differences with adults. Brain activation following tendon vibration at 100 Hz ('illusion') and 30 Hz ('no illusion') were analysed using the two-stage random effects model, with or without white and grey matter covariates. The BRS was already well established in children as revealed by the contrast 'illusion' vs 'no illusion', although still immature in some aspects. This included a lower level of activation in primary somatosensory and posterior parietal regions, and the exclusive activation of the frontopolar cortex (FPC) in children compared to adults. The former differences were related to structure, while the latter difference reflected a functional strategy where the FPC may serve as the 'top' in top-down modulation of the activity of the other BRS regions to facilitate the establishment of body representations. Hence, the development of the BRS not only relies on structural maturation, but also involves the disengagement of an executive region not classically involved in body processing.

1. Introduction

Neural representations of the body formed within the human brain, known as the body representation system (BRS), is central to the understanding of motor functions (Ehrsson et al., 2003; Longo and Haggard 2010). The BRS is constantly updated using sensory information, especially proprioception that encompasses the perception of positional changes and movements of body parts (Proske and Gandevia, 2012). Using vibration-evoked proprioceptive illusions, neuroimaging studies suggested that two networks constitute the cerebral basis of the BRS (Naito et al., 1999, 2002, 2016; Naito and Ehrsson, 2006): (i) a sensorimotor control network – i.e. motor and somatosensory cortical regions, basal ganglia, thalamus, cerebellum – that contributes to the formation of the body representations, and is involved in on-line control (fast corrections) of movement, and (ii) a fronto-parietal network extending from the inferior frontal gyrus to the posterior parietal cortex (e.g. inferior parietal lobule) that integrates environmental information together with bodily information into a single percept, thereby providing a corporeal representation adjusted to the environmental context. Furthermore, the fronto-parietal network in the right hemisphere has also been found to be involved in corporeal self-awareness (Cignetti et al., 2014; Naito et al., 2005). Although it is obvious that the BRS must be updated during development due to many factors such as morphological changes, acquisition of motor skills, and cognitive practice, age-related changes in its cerebral correlates have never been investigated directly.

Indirect information on the developmental trajectory of the BRS comes from resting state functional magnetic resonance imaging (fMRI) studies. The sensorimotor control network is already topologically adult-like by the age of two while higher-order networks including the fronto-parietal network are topologically incomplete, presenting a less specialized architecture compared to adults (Gao et al., 2015). Further studies reported that within-network connectivity changes stop in late childhood (~10 years old) for the sensorimotor network and that they continue until adulthood for the frontal and parietal networks (Jolles et al., 2011; Kelly et al., 2009). Therefore, the fronto-parietal network supporting the BRS presents an extended development compared to the sensorimotor network. A recent fMRI study using tendon vibration also demonstrated that the proprioceptive brain network still undergoes refinements during and beyond adolescence, mostly the fronto-striatal connections that exhibit functional pruning leading

* Corresponding author at: Aix Marseille Univ, CNRS, LNC, Laboratoire de Neurosciences Cognitives, Marseille, France.
E-mail address: christine.assaiante@univ-amu.fr (C. Assaiante).

https://doi.org/10.1016/j.dcn.2017.02.010

to a more restricted topology (Cignetti et al., 2016a). Therefore, although the sensorimotor network is likely earlier to mature compared to the fronto-parietal network, it may not yet be mature by late childhood.

Outcomes from structural MRI studies would support this view. Studies on cortical grey matter development from childhood to adulthood reported a maturational sequence from sensorimotor to higher-order association regions, specifically from the precentral gyrus to the prefrontal cortex in the frontal lobe and from the postcentral gyrus to the angular/supramarginal gyri in the parietal lobe (e.g. Gogtay et al., 2004; Shaw et al., 2008). Likewise, a study by Zielinski et al. (2010) showed that grey matter networks establishing sensory and motor regions were already well-developed in early childhood, although not yet adult-like. In contrast, higher-level cognitive networks were undeveloped in early childhood and showed an important amount of change during adolescence. However, regional variations in the grey matter maturation pattern of the sensorimotor network appear to exist, especially in the subcortical regions that demonstrate important age-related changes in grey matter density during adolescence (Sowell et al., 1999).

Considering white matter maturation, it is less clear whether the sensorimotor network reaches maturity before the fronto-parietal network. Diffusion tensor imaging (DTI) studies showed that the microstructural characteristics of association fibres, and especially the superior longitudinal fasciculus that connects the parietal cortex to the frontal gyrus, become adult-like by late adolescence (Asato et al., 2010; Lebel et al., 2008, 2012; Lebel and Beaulieu, 2011; Simmonds et al., 2014). This supports an extended development of the fronto-parietal network. However, late to mature in adolescence are also projection fibres, such as the corona radiatia connecting the basal ganglia to the cortex, as well as cerebellar connections (Asato et al., 2010; Lebel et al., 2008; Simmonds et al., 2014). Moreover, connections at terminal grey matter sites in basal ganglia were found to mature even in later adulthood (Lebel et al., 2008; Simmonds et al., 2014). Therefore, a set of white matter fibres involved in the sensorimotor network continue to mature during and beyond adolescence, suggesting once again that this network is not completely mature by late childhood.

Using a protocol of kinaesthetic illusions in children (7–11 years) and adults (25–40 years) in fMRI, the aim of the present study was to evaluate the degree of maturation of the sensorimotor and fronto-parietal networks subtending the BRS by late childhood. We expected to find larger differences in activation levels between children and adults in fronto-parietal regions, i.e. a more immature fronto-parietal network by late childhood. A secondary objective was to examine the extent to which structural brain maturation influences the functional development of the networks that implement the BRS. To this end, we investigated group differences in fMRI results while statistically controlling for differences in grey and white matter between children and adults.

2. Methods

2.1. Participants

Forty seven healthy right-handed individuals including fifteen adults (mean age ± SD: 32.4 ± 4.5; 9 females) and thirty two children (from seven to eleven years old) took part in the experiment. Data from 9 of the adult participants were previously reported by Cignetti et al. (2014) and six additional adult participants were recruited to complete the adult group. The children sample was finally restricted to twenty-two individuals (mean age ± SD: 9.0 ± 1.4; 15 females) due to the exclusion from the analysis of 10 children with excessive head movements during fMRI scanning (cf. Section 2.5.1 fMRI data analysis). Sex distribution did not differ between the two age groups (χ^2 (4, n = 37) = 0.3; p = 0.6). Adult participants, parents of minors, and children gave written informed consent. The study was approved by the research ethics committee CPP Sud-Méditerranée 1.

2.2. Paradigm

The cerebral correlates of the BRS were examined using a tendon vibration paradigm, which consisted in vibrating the tendons of the right and left tibialis anterior muscles to excite the muscle spindle primary endings (e.g. Cignetti et al., 2014, 2016a). To this end, custom-made pneumatic vibration devices, driven by constant air pressure, were placed perpendicularly to the anterior right and left ankles using elastic straps (contact area = ∼ 6 cm^2). Frequencies were delivered at 30 Hz and at 100 Hz with a 0.5 mm amplitude, leading to four vibration conditions: right and left tendon vibration at 30 Hz (R30 and L30; the control 'no illusion' condition) and at 100 Hz (R100 and L100; the 'illusion' condition). These stimulation parameters were selected based on the fact that (i) 20–40 Hz frequencies drive weak discharges of the primary endings, which are not likely to elicit kinaesthetic illusions, and (ii) ∼100 Hz frequency optimally activates primary endings, generally providing consistent illusory movements (i.e. plantar-flexion) (Cignetti et al., 2014, 2016a; Naito et al., 1999; Radovanovic et al., 2002; Roll and Vedel, 1982; Roll et al., 1989).

2.3. Pre-scanning session

In the present study, participants first experienced a pre-scanning session lying supine outside the scanner with the eyes closed, during which they were presented with the four vibratory stimulations (12-s long R30, L30, R100, and L100 vibrations; each stimulation presented twice). The vibration conditions were presented in a random order and each vibration was followed by a rest period during which the participants were questioned as to whether the stimulation generated illusory movements, and were then requested to verbally describe them. The six additional adults reported illusory movement at 100 Hz but not at 30 Hz stimulation. Finer-grained evaluation was conducted in children to increase confidence in self-reports on illusions. After the 12 seconds period of vibration, the children had to report about what they felt and were asked to reproduce (if any) the illusory percept by moving their foot. In the 100 Hz condition, all children felt their foot 'going down' and produced a plantar-flexion. In the 30 Hz condition, 6 children reported plantar-flexion illusion while the other 16 children reported a 'vibrating' sensation. Children were also asked to (i) score the vividness defined as how realistic the illusion was, between 0 and 4, a score of 0 corresponding to the absence of illusion and a score of 4 to a plantar-flexion illusion similar to an actual movement (Naito et al., 1999), and (ii) to report the amplitude of the illusory movement, using an angle measurement scale. The angle measurement scale corresponded to a lying individual with a degree of freedom about the ankle. The experimenter rotated the foot until the estimated position was reached, as indicated by the children. An angle of 0° corresponded to the absence of illusory plantar-flexion and a positive value to a plantar-flexion, the larger the value the more important the plantar-flexion. In sum, none of the adults reported experience of illusory movement in the 30 Hz conditions while all of them experienced illusory plantar-flexion in the 100 Hz conditions. Six children out of twenty-two reported illusory movements in both the 30 Hz and the 100 Hz conditions, with a tendency for less vivid and important illusions in the former conditions (vividness R30: 1.5 ± 1.4; vividness L30: 1.3 ± 1.2; angle R30: 17.5 ± 10.3°; angle L30: 19.2 ± 9.3°) compared to the latter conditions (vividness R100: 2.5 ± 1.4, L100:

3 ± 1; angle R100: 25.2 ± 10.3°, L100: 23.5 ± 13.8°). The other 16 children reported illusions in the 100 Hz conditions only (vividness R100: 2.8 ± 0.7, L100: 3.1 ± 0.7; angle R100: 13.6 ± 2.9°, L100: 18.5 ± 5.1°).

2.4. MRI data acquisition

After the familiarization pre-scanning session, the subjects were placed head first and supine into a 3T MRI scanner (Medspec 30/80 AVANCE, Bruker, Ettlingen, Germany). Supports were used to minimize head movement, including a soft strap attached around the head and air pads placed between the lateral sides of the head and the radio-frequency head coil. The participants also wore a headphone for communication purpose. fMRI time series were acquired with a T2*-weighted gradient echo-planar imaging sequence (42 interleaved axial slices acquisition; 3 mm thickness; 0.5 mm interslice gap; reconstruction matrix = 64 × 64; field of view = 192 mm × 192 mm; repetition time = 2.8 s; echo time = 30 ms; flip angle = 84°). The scanning planes were parallel to the anterior commissure – posterior commissure and covered the top of the cortex down to the base of the cerebellum. The scanning session was composed of five runs each lasting 5 min and including 12-s long conditions (epochs) of vibration (R30, L30, R100, L100) and REST. Each vibration condition was repeated three times per run. The order of vibration conditions was randomized within a run, and REST epochs were inserted between all vibration conditions to ensure the relaxation of the muscle spindles. At the end of each run, subjects were questioned about the illusory movements via headphones. For each stimulation condition, we asked whether it induced illusory movements, and if yes, whether all three repetitions (each stimulation condition having been repeated three times within a run) induced illusory movements. Subjects answered the questions using a finger button response system. Answers were identical to the verbal report of the pre-scanning session for all participants. The six additional adults and all children reported consistent illusion for the R100 and the L100 in all runs. In addition, the six children who reported having experienced an illusion at 30 Hz during the pre-scanning phase also reported consistent illusory movements for the R30 and L30 stimulation in all runs. We preferred asking the subjects to report the presence of illusions after each run instead of after each stimulation to avoid methodological issues related to movement preparation. Indeed, reporting illusions on an epoch basis would have involved pre-movement activity of the responding finger in areas that were processing proprioceptive information, including precentral and parietal areas (Mars et al., 2008; Rushworth et al., 2003; Toni et al., 1999).

Structural MRI data were also acquired using a 12 min three-dimensional T1-weighted scanning sequence (MP-RAGE; repetition time = 9.4 ms; echo time = 4.4 ms; inversion time = 800 ms; field of view = 179 mm × 256 mm × 180 mm, reconstruction matrix = 256 × 256 × 180). Finally, the participants underwent an 8 min MR-diffusion scanning. MR-diffusion images were acquired using a dual spin-echo, single shot echo-planar imaging sequence (TE = 86.659 ms; TR = 10400 ms; 52 axial slices, 2.3 mm thickness, without gap; field of view = 242 mm x 242 mm and matrix size = 128 × 128). Each MR-diffusion data set included 8 non-diffusion-weighted and 36 diffusion-weighted images acquired with a b-value of 1000 s/mm^2.

2.5. Data analyses

2.5.1. fMRI

Image pre-processing and statistical fMRI data analysis were conducted with SPM8 (Wellcome Department of Imaging Neuroscience, London, UK) running in Matlab 7.5 environment (Mathworks, Inc., Sherbon, MA, USA) and custom-made Matlab scripts. Each run included 113 images, including six dummy images of magnetic field saturation that were discarded. The remaining images were first (i) slice-time corrected, (ii) realigned to the first image of the time series to correct for head movement between scans, (iii) unwrapped to remove residual movement-related variance (Andersson et al., 2001), and (iv) co-registered to high-resolution structural data. The structural image was normalized to the MNI (Montreal Neurological Institute) T1 template image and the resulting parameters were used for normalization of the functional images, which were resampled to 3-mm isotropic voxel size and smoothed with an 8-mm FWHM Gaussian kernel. Ten children in which translational and rotational head movement as obtained from realignment (step ii) exceeded 3 mm and 3°, respectively, were discarded from the study. We applied this rule-of-thumb since higher amount of motion are not corrected properly by applying motion correction procedures (Formisano et al., 2005). Accordingly, the final children population considered for analysis included twenty two individuals.

Pre-processed data were afterwards analysed using the univariate two-stage summary statistics random effect model (Cignetti et al., 2016b; Friston et al., 1995; Holmes and Friston, 1998). Task-dependent changes in BOLD signal were modelled as box-car regressors time-locked to the onsets of the vibrations (R30, L30, R100, and L100) and REST conditions. These regressors were convolved with the canonical hemodynamic response function (HRF) of SPM8 and entered into the general linear model (GLM). Constant terms and parameters for head movement estimated by motion realignment procedure were entered at the individual level as covariates of no interest to account for shifting signal levels across runs and influence of head motion on BOLD signal, respectively. Specifically, a 24-parameter autoregressive model including current and past position parameters along with the square of each parameter was used to account for the cumulative effects of motion on spin magnetization (Friston et al., 1996). It has been demonstrated that this modelling-based strategy is the most efficient to account for motion-related variations in the BOLD signal (Yan et al., 2013). Finally, a high-pass filter (cut-off period = 128 s) was applied to remove low-frequency drifts in the data. Maps of parameter estimates were computed from the GLM to reveal the magnitude of activation of the regions subtending the BRS, i.e. individual SPM{t} maps of the contrast RL100 (illusion condition) > RL30 (no illusion condition). Note that such contrast pooled the right and left stimulations. Individual maps were then entered into a second-level random-effects GLM to evaluate group differences. A summary measure of head motion (i.e. mean framewise displacement, labelled mean FD) was also included as a covariate in the second-level random-effects GLM. The mean FD was continuous and corresponded to the mean head displacement over the 5 functional runs and was calculated as the summed absolute values of the derivatives of the translational and rotational realignment estimates (after converting rotational estimates to displacement at 50 mm radius; Power et al., 2012), averaged over all scans. Associating subject-level correction with the realignment parameters and group-level correction for mean FD appears to be an optimal strategy to regress out motion-related artefacts from the data (Fair et al., 2013; Yan et al., 2013). Multiple comparisons correction of statistical maps at the second-level was conducted using a cluster-based extent thresholding of $p < 0.05$ (FWER-corrected) calculated based on the Gaussian random field method and following a primary threshold set at $p < 0.005$. We set the primary threshold at a relatively liberal threshold given that our working hypotheses dealt with large-scale networks (i.e. fronto-parietal network and motor network including cortical and subcortical structures), or equivalently large clusters of activation, and not anatomically localized activity pattern (Woo et al., 2014).

The extent to which brain structure influenced BOLD contrast differences between the two groups was examined from individual white (DTI) and grey (grey matter mask from T1 scan) matter information implemented into the second-level random effects GLM as covariates, thereby adjusting functional results for structural differences between children and adults. Details on how these covariates have been obtained are provided below.

2.5.2. White matter

Processing of MR-diffusion data was conducted using tools in FSL5.0 (Smith et al., 2004). As a first step, non-brain tissues were deleted from diffusion- and non-diffusion-weighted images (BET tool; Smith, 2002) and diffusion-weighted images were aligned to the first non-diffusion-weighted image using affine registration (FLIRT tool; Jenkinson et al., 2002). Affine registration was used to reduce misalignment between the images due to head motion and eddy currents. The effects of subject motion on diffusion-weighted images were assessed afterwards using the procedure developed in Yendiki et al. (2014), which relied on four different measures: (i) the average image-by-image translation, (ii) the average image-by-image rotation, (iii) the percentage of slices with signal drop-out, and (iv) the signal drop-out severity. The average image-by-image translation and rotation indicated acceptable (i.e. ~3 mm translation and ~3° rotation) between-image motion in all subjects. These four measures enable the capture of the global frame-to-frame motion as well as the frequency and severity of rapid slice-to-slice motion, and was used to detect volume data corrupted by motion. In particular, one image among the 36 diffusion-weighted images demonstrated more than 5% of drop-out for three children. These images were therefore removed from subsequent analysis. Finally, a tensor model was fit to the images (DTIFIT tool) at each voxel and the fractional anisotropy (FA) was obtained voxelwise. FA images of each participant were aligned to a standard space (FMRIB58 FA image) using a nonlinear registration and then, using an affine registration, aligned to the MNI152 template.

Individual FA values were finally extracted from 8 tracts of interest (averaged over the left and right hemispheres for each tract) of the Johns Hopkins University (JHU)-ICBM-DTI-81 white matter labels atlas (Mori et al., 2008; Wakana et al., 2007). These tracts included association (i.e. corticospinal tract, corona radiata, external capsule, cingulum, superior longitudinal fasciculus, and superior fronto-occipital fasciculus) and projection (i.e. anterior limb of the internal capsule) fibres as well as cerebellar pathway (i.e. cerebral peduncle) that interconnect the different cortical, subcortical and cerebellar regions most likely involved in BRS processing. Finally, the set of FA values were decomposed into principal components and the first component (accounting for 67% of variance; Fig. 1) served as the covariate that was carried forward to the second-level GLM analysis of fMRI data.

2.5.3. Grey matter

Grey matter information was obtained using voxel-based morphometry (Ashburner and Friston, 2000; Good et al., 2001) implemented in VBM8 toolbox. As a first step, all T1 images were inspected for artefacts and the centre point was placed on the anterior commissure. All images were subsequently (i) normalized (affine registration) to the MNI152 standard space (using a Bayesian framework), (ii) segmented in grey matter, white matter and cerebro-spinal fluid partitions, and (iii) smoothed with an 8-mm FWHM Gaussian kernel. Grey matter density (dGM) was extracted from regions of interest (ROIs) of the probabilistic Harvard-Oxford cortical and subcortical structural atlases that cover 48 cortical and 21 subcortical structural areas (Desikan et al., 2006; Makris et al., 2006). Specifically, individual dGM was obtained from fourteen ROIs (averaged over the left and right hemispheres for each ROI) that most likely compose the sensorimotor and the fronto-parietal networks of the BRS, including the inferior frontal gyrus, the insular cortex, the caudate, the putamen, the thalamus, the parietal operculum, the postcentral gyrus, the precentral gyrus, the cingulate gyrus, the superior parietal lobule, the precuneus, the superior frontal gyrus, the prefrontal cortex, and the middle frontal gyrus. As for the white matter, principal component analysis was finally run to decompose the set of dGM values. The first component accounted for 65% of variance of the data set (see Fig. 1), and served as the covariate in second-level GLM analysis of fMRI data.

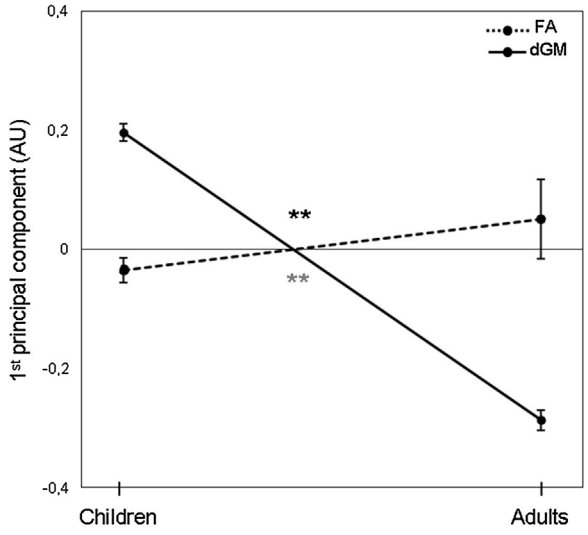

Fig. 1. Grey and white matter maturation. Mean ± SE of the first principal component (1st PC) for FA (filled line) and dGM (dashed line) for the children and the adults. The 1st PC accounted for 67% and 65% of the variance of the FA and dGM data sets, respectively. Group comparison revealed a significant difference both for FA and dGM ($t_{35} = -3.8$ and $t_{35} = 7.9$; $^{**}p < 0.001$, respectively), reflecting an increase of the FA and a decrease of the dGM with age. FA: fractional anisotropy; dGM: grey matter density.

3. Results

3.1. Brain regions contributing to the BRS in children and adults

The RL100 > RL30 contrast, or equivalently the comparison between the illusion and the no illusion conditions, revealed significant activations ($p < 0.05$ FWER-corrected) in several cortical and subcortical areas for both groups (Fig. 2). As illustrated in Fig. 2, clusters of activation were located in the basal ganglia (putamen, caudate) and neighbouring regions (claustrum, anterior insula), motor-related regions (anterior cingulate cortex – BAs 24 and 32, supplementary motor area – BA 6, primary somatosensory cortex – BA 3), and associative regions (inferior frontal gyrus – BA 44, and inferior parietal lobule – BA 40) in the two hemispheres. These results support the idea that both the sensorimotor and the frontoparietal regions are already contributing to processing bodily information in late childhood. Detailed information on the clusters of activation (spatial localization, number of active voxels, intensity) are provided in Table 1.

Yet, the spatial extent of the pattern of the children's network was larger than in the adult's network (Table 1). Visual inspection of Fig. 2 clearly highlights such difference between children and adults. Moreover, a significant cluster of activation was found in the frontopolar cortex (BA 10) in the children only (cf. top part of Fig. 2).

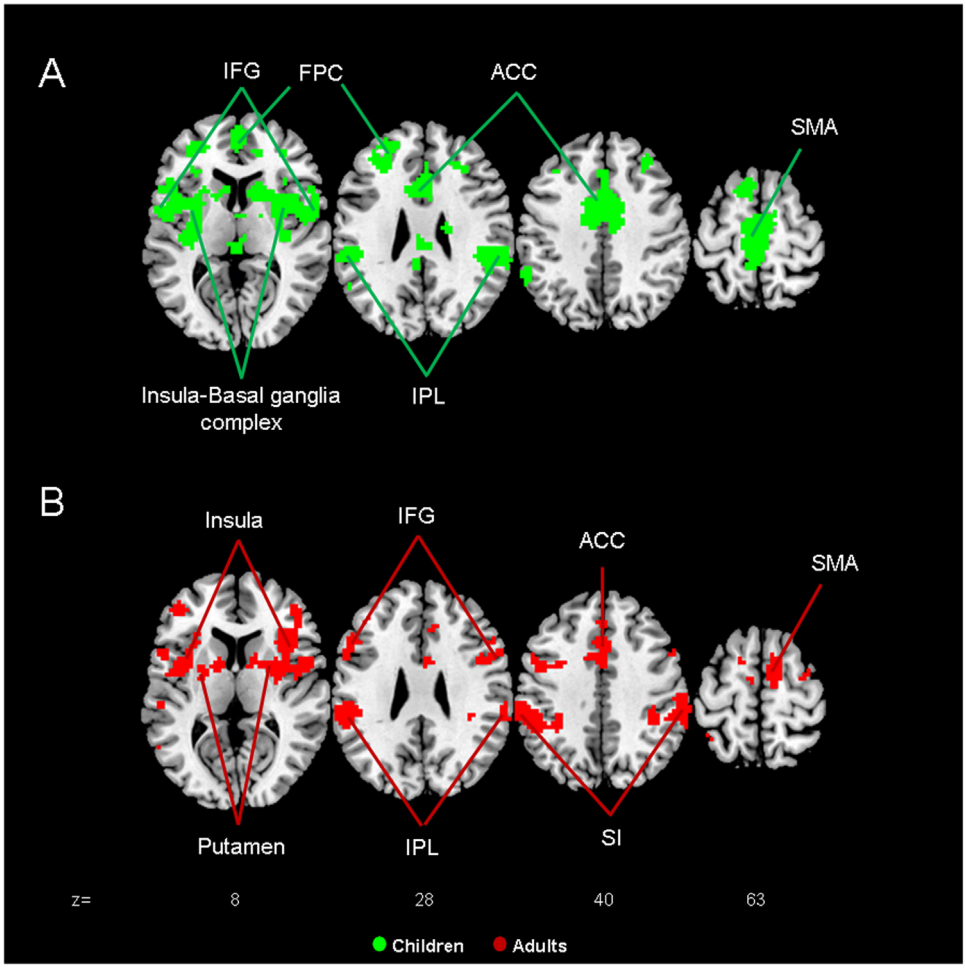

Fig. 2. Activation maps for the RL100 > RL30 contrast for (A) the children (green) and (B) the adults (red). Maps are thresholded at $p < 0.05$ family-wise error rate (FWER)-corrected with cluster-based extent thresholding at $p < 0.005$ and $k = 20$ voxels.
IFG: inferior frontal gyrus; FPC: frontopolar cortex, IPL: inferior parietal lobule, ACC: anterior cingulate cortex, SI: primary somatosensoy cortex; SMA: supplementary motor area. The Insula-Basal ganglia complex involved the right and left anterior insula, putamen, and caudate. This complex also overlapped with the claustrum in both right and left hemisphere.

3.2. Differences in brain activation with age

Contrast between children and adults (i.e. Children > Adults) revealed a significant cluster in the frontopolar cortex (Fig. 3A; Table 2). This is a direct consequence of the exclusive activation of this region in children relative to adults previously reported. The inverse contrast, namely Adults > Children, revealed two significant clusters with activation peaks localized in the right and left inferior parietal lobules and primary somatosensory cortices (Fig. 3B; Table 2). As showed by the barplots of Fig. 3B, which represent the percent signal change (PSC) in the RL30 and RL100 conditions for the activation clusters, the PSC in the adults was found to be lower in the RL30 condition compared to the RL100 condition while there was no clear PSC difference between both conditions in the children. The RL30 condition seems to elicit for those regions a ceiling effect on the BOLD signal in children. Altogether, these results indicate an immaturity of the BRS in late childhood that manifests at the brain level through (i) the additional recruitment of a prefrontal region to the sensorimotor and fronto-parietal networks, and (ii) a parietal activation less sensitive to variations in proprioceptive inputs (i.e. a ceiling effect for weak discharges of primary endings).

Correction of the fMRI results for the white matter or the grey matter (i.e. FA or dGM used as the covariate in second-level fMRI analysis, respectively) still revealed the cluster of activation in the frontopolar cortex that initially resulted from the contrast Children > Adults. However, a substantial reduction of the cluster size was induced by the dGM correction (Fig. 4, Table 2). Hence, the functional difference between children and adults with respect to this cluster is not simply explained by structural maturation, although changes in local grey matter density with age contributes to the effect. Inversely, clusters found using the contrast Adults > Children, whose activation spread over the primary somatosensory cortices and the inferior parietal lobules, did not remain significant when using either FA or dGM as a covariate in the analysis. Therefore, functional differences between the two groups about the parietal cortex emerge as a consequence of structural maturation.

3.3. Supplementary analyses

Since the children group included six individuals who reported illusions in the 30 Hz condition (i.e., a 'biased' control condition) and was therefore not as homogeneous as the adult group, we replicated the previous group-level analyses removing these children. Both the RL100 > RL30 contrast in children (see supplementary Fig. 1 and Table 1) and group comparisons (see supplementary Fig. 2 and Table 2) revealed similar statistical parametric maps as those previously observed with the 22 children. Thus, we are confident in saying that second-level outcomes reflected differences between a no illusion condition and an illusion condition, therefore providing

Table 1
Activation peaks during right and left vibratory stimulus (RL100 > RL30 contrast) for adults and children. Z-values refer to significant activation peaks at $p < 0.005$ (uncorrected for multiple comparisons). All cluster reported are significantly active at $p < 0.05$ (FWER-correction). Coordinates are reported in the MNI space; L: left hemisphere, R: right hemisphere.

RL100 > RL30							
	Peak location	BA	Side	x(mm)	y(mm)	z(mm)	z-values
CHILDREN	Cluster # 1(3751 voxels)						
	Insula	13	L	−39	2	13	6.07
			R	45	−1	13	5.56
	Ant. Cing. Gyrus	24	R	6	−7	46	5.75
			L	−6	−7	43	5.46
	Precentral Gyrus	44	L	−51	−1	10	5.67
	Primary Motor Area	4	L	−6	−34	70	5.63
	Sup. Motor Area	6	L	−3	−19	73	5.61
	Claustrum		R	33	−1	13	5.49
	Inf. Parietal Lobule	40	R	60	−34	31	5.32
			L	−51	−31	25	4.99
	Sup. Front Gyrus	6	L	−9	−19	76	5.23
	Cluster # 2(227 voxels)						
	Frontopolar Cortex	10	L	−30	44	4	4.91
		9	L	−30	35	31	4.39
	Cluster # 3(99 voxels)						
	Inf. Front. Gyrus	44	R	33	41	1	4.07
	Ant. Cing. Cortex	32	R	15	44	7	3.13
	Frontopolar Cortex	10	R	15	56	−2	2.97
ADULTS	Cluster # 1(558 voxels)						
	Inf. Parietal Lobule	40	L	−51	−34	22	6.07
			L	−51	−31	34	4.28
	Postcentral Gyrus	1;2	L	−60	−28	40	3.87
	Cluster # 2(884 voxels)						
	Insula	13	R	36	23	1	4.93
	Precentral gyrus	44	R	54	5	10	4.90
	Claustrum		R	33	−1	10	4.70
	Inf. Frontal Gyrus	44	R	54	11	22	3.96
	Putamen		R	24	8	1	4.30
	Cluster # 3(568 voxels)						
	Insula	13	L	−42	−1	10	4.65
	Inf. Frontal Gyrus	44	L	−57	14	28	4.53
	Putamen		L	−27	−13	16	3.88
	Middle Frontal Gyrus	6	L	−45	2	43	3.87
	Claustrum		L	−30	20	4	3.86
	Precentral Gyrus	44	L	−54	11	7	3.79
	Cluster # 4(317 voxels)						
	Inf. Parietal Lobule	40	R	39	−37	40	4.5
			R	63	−34	31	4.28
	Postcentral Gyrus	1;2	R	63	−25	40	4.35
	Cluster # 5(317 voxels)						
	Sup. Motor Area	6	L	−3	11	49	4.04
			R	6	2	58	3.17
	Ant.Cing. Cortex	24;32	L	0	20	43	3.78
			R	3	5	31	3.68

relevant information on the BRS (i.e. mapping sensory inputs into body representations).

4. Discussion

Using kinaesthetic illusions in fMRI, the present study investigated the degree of maturity of the sensorimotor and fronto-parietal networks implementing the BRS by late childhood, with the assumption that larger differences in activation should be about regions of the latter network when comparing children to adults. A secondary objective was to investigate the causes of age-related changes in functional activation by examining the extent to which maturational changes in white and grey matter account for it. Overall, the results showed similar brain activation patterns in adults and children involving sensorimotor (SMA, basal ganglia) and fronto-parietal (IPL, IFG) regions, although the spatial extent of activation was larger in the children (i.e. more diffuse activation). Such a shift from more diffuse to more focal cortical activity appears to be a general principle of brain development (Casey et al., 2005; Cignetti et al., 2016a; Durston et al., 2006). Outcomes are twofold with regard to group differences, involving (i) a more intense activation in the right and left inferior parietal lobules and primary somatosensory cortices in the adults compared to the children, and (ii) the additional engagement of a prefrontal region (frontopolar cortex, BA10) in children. Altogether, these findings suggest that while the basic configuration of the sensorimotor and fronto-parietal networks of the BRS is established by the age of 7–11, functional specialization of both networks – and not only of the fronto-parietal network – continue during adolescence. Importantly, such functional specialization is fully explained by structural grey and white matter maturation for the parietal/somatosensory regions but not for the prefrontal region.

4.1. Age-related changes in somatosensory and parietal activations

The higher magnitude of activity in adults compared to children, as reported here both in the primary somatosensory and inferior parietal lobule regions, is commonly interpreted as immature neural mechanisms not processing as efficiently as they do in

Table 2
Activation peaks for the contrast Children > Adults (top) and Adults > Children (bottom) with and without correction for group differences in white (FA) and grey (dGM) matter. Z-values refer to significant activation peaks at $p < 0.001$ (uncorrected for multiple comparisons). All cluster reported are significantly active at $p < 0.05$ (FWER-correction). Coordinates are reported in the MNI space; L: left hemisphere, R: right hemisphere, FA: fractional anisotropy, dGM: grey matter density.

CHILDREN > ADULTS							
	Peak location	BA	Side	x(mm)	y(mm)	z(mm)	z-values
fMRI	Cluster # 1 (480 voxels)						
	FrontoPolar Cortex	10	L	0	53	7	4.38
			R	15	56	4	3.03
fMRI-FA	Cluster # 1 (511 voxels)						
	FrontoPolar Cortex	10	L	0	53	7	4.35
			R	−3	56	−8	4.22
			R	6	53	−5	4.22
fMRI-dGM	Cluster # 1 (147 voxels)						
	FrontoPolar Cortex	10	L	−12	53	19	3.77
			R	9	50	7	3.74
			R	3	56	13	3.60
ADULTS > CHILDREN							
fMRI	Cluster # 1 (327 voxels)						
	Postcentral gyrus	1; 2	L	−57	−28	40	4.63
	Inf. Parietal Lobule	40	L	−36	−43	52	4.00
	Cluster # 2 (143)						
	Inf. Parietal Lobule	40	R	39	−34	40	5.57
			R	51	−34	40	4.39
	Postcentral Gyrus	3	R	60	−25	40	5.17

The significant clusters reported in fMRI did not survive to correction for group differences in grey and white matter.

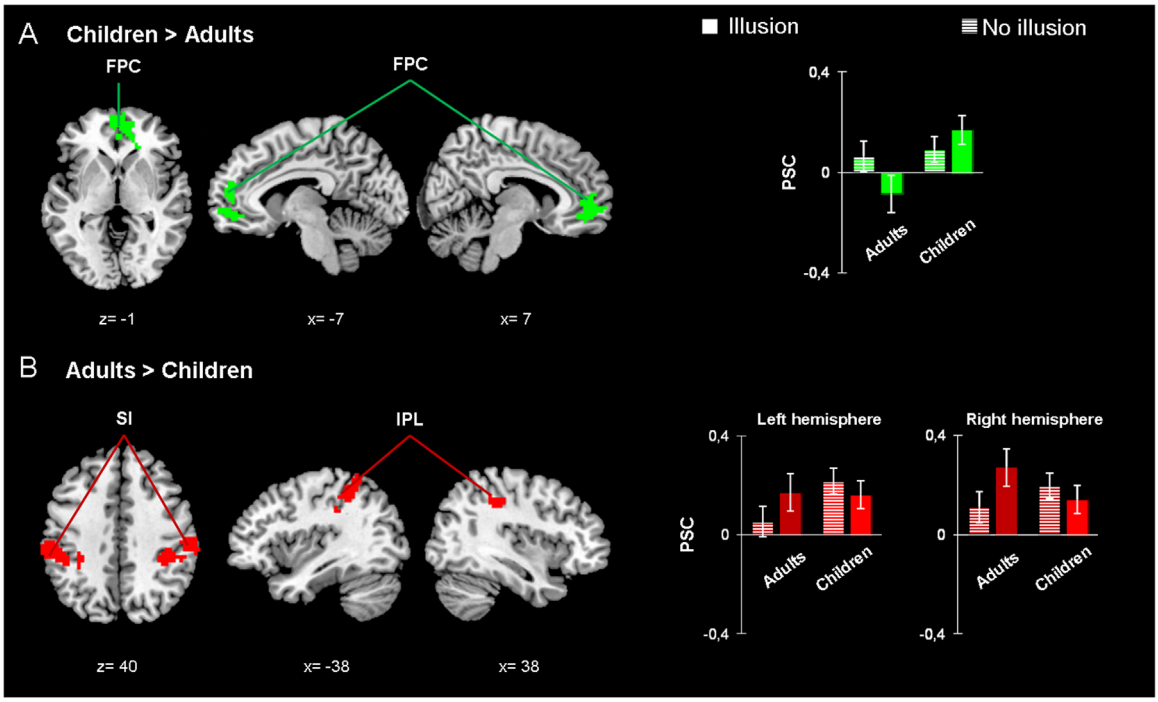

Fig 3. Comparison of the adults and children group activity for the RL100 > RL30 contrast. A: Children > Adults contrast (Green) and B: Adults > Children contrast (Red). Maps are thresholded at a voxel-wise threshold of $p < 0.001$ uncorrected and a cluster extend threshold of $p < 0.05$ FWE-corrected. Barplots show the percent of signal change (PSC) ± SE for each significant cluster. PSC were extracted using MarsBaR (Brett et al., 2002). Dashed bars represent the RL30 condition and filled bars the RL100 condition. FPC: Frontopolar Cortex, SI: Primary Somatosensory Cortex; IPL: Inferior Parietal Lobule.

the mature system (Luna et al., 2010). Accordingly, this finding suggests that children were not able to access a mature and presumably optimal processing in these regions related to BRS and corporeal awareness. Indeed, there is ample evidence that the posterior parietal cortices, and especially the inferior parietal lobules, in the two hemispheres play a crucial role in monitoring/sustaining body representations (see Daprati et al., 2010 and Naito et al., 2016 and references therein) and accessing consciously to these representations (Cignetti et al., 2014; Desmurget et al., 2009; Desmurget and Sirigu, 2009). Likewise, several works support the idea that body representations are hosted within the primary somatosensory cortices (Ehrsson et al., 2005; Blakemore et al., 1998). A study by Di Russo et al. (2006) even reported cortical modifications in both the primary somatosensory cortex and in the posterior parietal cortex following surgical extension of the lower limbs. Although crucial to body representations, the primary somatosensory cortex and the posterior parietal cortex also likely play different roles, the latter region being more concerned with higher-order aspects related to

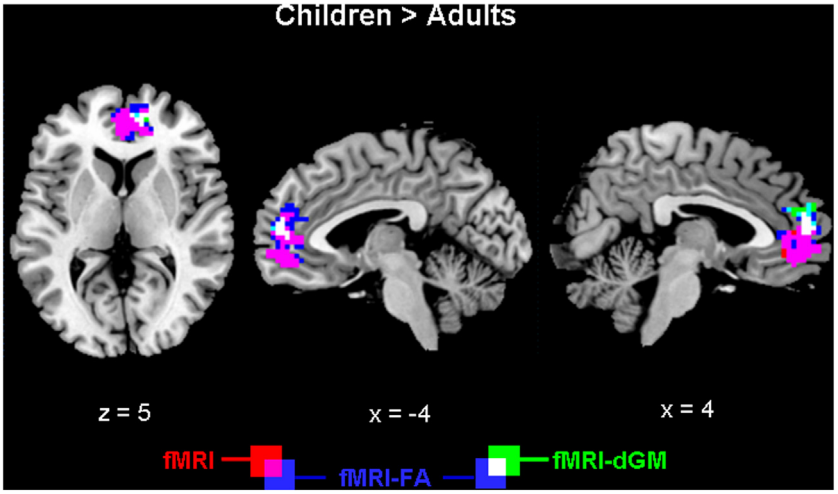

Fig. 4. Activation cluster in the frontopolar cortex revealed by the contrast Children > Adults (red) corrected for differences with age in FA (blue) and dGM (green). Voxel-wise threshold was set at $p < 0.001$ uncorrected and cluster extend threshold at $p < 0.05$ FWE-corrected.

the body such as awareness and updating body representations according to the environment (Berlucchi and Aglioti, 1997; Naito et al., 2016). The examination of the PSC provided further information about how to interpret the above developmental regional difference. The less marked increase in PSC from the RL30 condition to the RL100 condition in children compared to adults suggested a lower ability in the former to discriminate between sensory inputs, or equivalently to map them into accurate body representations. This interpretation is also consistent with behavioural findings that show a lower ability of the children compared to the adolescents and the adults to estimate limbs' positions using proprioception (Goble 2010; Goble et al., 2005). However, it doesn't coincide with the children's behavioural outcomes. Indeed, children reported to experience illusory movement at 100 Hz, and few or none of them reported illusory movement at 30 Hz. This suggests a perceptual sensibility at a behavioural level which is not reflected by the parietal activity. Nevertheless, the focus on the posterior parietal areas activation assessment appears insufficient to completely explain the functional correlates eliciting illusory movement. Therefore, a more complete vision covering the functional connectivity within the BRS would be required in order to capture the generalization of illusory processes in its entirety (Hagura et al., 2009)

More importantly, the increase with age in the magnitude of activation within these two regions disappeared when accounting for grey and white matter. Such a relationship between structure and function in the parietal cortex is not surprising given the significant changes that occur in its structural morphology during adolescence. There is evidence for a significant decrease in grey matter density and thickness in the parietal cortex starting at about 10 (e.g. Gogtay et al., 2004; Shaw et al., 2008), which support the development of mature activation patterns. For instance, several studies have shown that increased activation over development is accounted for by cortical thinning (Lu et al., 2009; Wendelken et al., 2011). White matter tracts also become more structured and myelinated with development to support higher efficiency of signal propagation, and thus improve information transfer between distant regions (Paus, 2010). In particular, certain association fibres that pass through the parietal lobe, such as those of the superior longitudinal fasciculus that plays a role in corporeal awareness (Amemiya and Naito, 2016), are still immature during adolescence (Asato et al., 2010; Lebel and Beaulieu, 2011). In sum, our study suggests a substantial influence of the brain structure to the development of the BRS network.

4.2. Disengagement of the anterior prefrontal cortex with development

Another important finding was the disengagement of the frontopolar cortex from the BRS from late childhood to adulthood. The frontopolar cortex is an anterior prefrontal region that forms the apex of the executive function system in humans (e.g. Miller and Cohen, 2001; Koechlin and Hyafil, 2007). This region has been reported to contribute to several high-level functions including motor intention, motor imagery, and decision making (Hilgenstock et al., 2014; Raos and Savaki 2016; Ludwig et al., 2015), and hence a supervisory function. Along this line, it has been shown that the prefrontal cortex modulates the magnitude of neural activity in distant brain regions – a mechanism of control known as top-down modulation – to establish high fidelity representations of task-relevant stimuli and to facilitate their internal maintenance (Gazzaley et al., 2007; Gazzaley and D'Esposito, 2007). Accordingly, the frontopolar cortex may serve in children as the 'top' in top-down modulation of the activity of the other BRS regions to facilitate the establishment of body representations from sensory (here, proprioceptive) inputs. This would signal a transition over the course of development from a rather top-down control scheme to a more bottom-up (i.e. automatic) control scheme for the generation of body representations from sensory inputs. Although the most common finding is an increase in activation of prefrontal regions with the development of cognitive control (Luna et al., 2010), our finding fits with previous evidence that some prefrontal regions show an age-related decrease in activation likely reflecting a decreased 'effort' required to exert cognitive control (Tamm et al., 2002).

Moreover, the frontopolar cortex is robustly involved in learning new behavioural cognitive sequences and progressively disengages over the course of learning (Koechlin et al., 2002). Specifically, this region disengages once an expectation or equivalently an internal representation has become reliable for a given sequence. Likewise, activation of the frontopolar cortex in children may relate with uncertain body representations given the proprioceptive inputs, and progressively disengages until adulthood as the amount of uncertainty related to mapping sensory inputs into body representation decreases. Again, this supports the idea that the activation of the anterior prefrontal cortex in children is an 'add-on' to the BRS system, perhaps to assist the other regions in building the more plausible representation given the ongoing sensory inputs.

Finally, the disengagement of the frontopolar cortex also marks a BRS system that becomes more segregated (or differentiated)

with development, which is a well-established principle of brain development (e.g. Cignetti et al., 2016a; Fair et al., 2007; Qin et al., 2012). Phenomena such as myelination, synaptic pruning and experience-dependent regional specialization are candidates to explain the increased segregation of cortical systems. Here, using white and grey matter as covariates still revealed frontopolar activation in the children. Therefore, disengagement of this region may be more related to experience-dependent changes in the activation of the BRS system. However, disambiguating structural from functional factors is difficult in that evoked activity plays a key role in determining which synaptic connections persist and which are eliminated during development (Changeux and Danchin 1976; Innocenti and Price 2005; Rakic et al., 1994, 2009). Accordingly, stating that the age-related disengagement of prefrontal activation is completely unrelated to structural factors is likely too simplistic. This is also supported by the fact that grey matter correction affected the prefrontal activation.

4.3. Methodological considerations

Although the study makes a unique contribution to the understanding of the maturation of the BRS and of the structural factors that influence it, methodological considerations have to be notified. First of all, six children experienced unanticipated illusory movements during the 30 Hz stimulation condition, indicating that the control condition included to some extent a body representation component and therefore may not have been optimal to investigate the BRS. However, we replicated group-level results when removing those subjects with illusory movements at 30 Hz. Accordingly, we are confident in saying that 100 Hz tendon stimulation vs. 30 Hz tendon stimulation was an adequate contrast to tap into the BRS, although the frequency difference between the two conditions also embedded a proprioceptive component. Another possibility would have been to contrast the 100 Hz tendon stimulation with a 100 Hz bone stimulation as done in previous studies (Goble et al., 2012; Naito et al., 2005). However, the resulting activations from this latter contrast would have been much more related to proprioceptive processing, making any conclusion of the BRS intricate.

Closely related to the previous issue was the absence of quantitative data about adult's illusory percept in our study. As a consequence, we could not have evaluated between-group difference in the extent to which amount of activation correlated with the degree of the illusion, which would have brought a finer-grained analysis of the cerebral correlates of body representations and the way these correlates develop. In particular, such an analysis would have been important to completely disentangle activations more related to the illusory percept from those more related to proprioceptive processing per se. Thus, it is of outmost importance that future investigations on the development of the BRS include careful psychophysical assessment of the illusion and link it to activation data.

Finally, the fact that we did not record electromyographic (EMG) activity during vibration may be considered a further limitation of our study. Indeed, vibration may have induced involuntary muscular contractions whose re-afferences might have blurred group results. However, previous studies reported either very limited EMG activity in a few subjects (e.g. Radovanovic et al., 2002) or no EMG activity (Naito et al., 1999; Amemiya and Naito 2016) during the vibratory stimulation. Therefore, this limitation is not likely to question the validity of the study outcomes.

5. Conclusion

Although the network subtending the BRS is already well established as early as 7–8, our study also demonstrated immaturity including a decreased activation in both sensorimotor (primary somatosensory cortex) and parietal (inferior parietal lobule) regions, as well as an exclusive anterior prefrontal (frontopolar) activation. The former differences were found to be entirely related to white and grey matter properties while the latter difference did not. This lends credence to the idea that maturation of the BRS network is complex and presents an extended development, relying on structural factors and a functional process that results in the disengagement of an executive region not classically involved in body processing. This expressed a functional neurodevelopmental strategy. Future studies will have to examine how the multimodal (i.e. modulation of proprioceptive-based representations by other sensory channels) and modular (i.e. interactions between brain regions) features of the BRS develop.

Conflict of interest

None.

Funding

This work was supported with funds from 'Fondation Yves Cotrel - Institut de France' and 'Fondation de France'.

Acknowledgements

The authors are grateful to the children, their parents, and the adults for their precious collaboration. The authors are also grateful to Doris Mathisen who revised the English.

Appendix A. Supplementary data

Supplementary data associated with this article can be found, in the online version, at http://dx.doi.org/10.1016/j.dcn.2017.02.010.

References

Amemiya, K., Naito, E., 2016. Importance of human right inferior frontoparietal network connected by inferior branch of superior longitudinal fasciculus tract in corporeal awareness of kinesthetic illusory movement. Cortex 78, 15–30, http://dx.doi.org/10.1016/j.cortex.2016.01.017.

Andersson, J.L., Hutton, C., Ashburner, J., Turner, R., Friston, K.J., 2001. Modeling geometric deformations in EPI time series. Neuroimage 13, 903–919, http://dx.doi.org/10.1006/nimg.2001.0746.

Asato, M.R., Terwilliger, R., Woo, J., Luna, B., 2010. White matter development in adolescence: a DTI study. Cereb. Cortex 20 (9), 2122–2131, http://dx.doi.org/10.1093/cercor/bhp282.

Ashburner, J., Friston, K.J., 2000. Voxel-based morphometry – the methods. Neuroimage 11, 805–821, http://dx.doi.org/10.1006/nimg.2000.0582.

Berlucchi, G., Aglioti, S., 1997. The body in the brain: neural bases of corporeal awareness. Trends Neurosci. 20 (12), 560–564, http://dx.doi.org/10.1016/S0166-2236(97)01136-3.

Blakemore, S.J., Wolpert, D.M., Frith, C.D., 1998. Central cancellation of self-produced tickle sensation. Nat. Neurosci. 1 (7), 635–640, http://dx.doi.org/10.1038/2870.

Brett, M., Anton, J.L., Valabregue, R., Poline, J.B., 2002. Region of interest analysis using an SPM toolbox [abstract]. Presented at the 8th International Conferance on Functional Mapping of the Human Brain, June 2–6, Sendai, Japan. Available on CD-ROM in NeuroImage, 16 (2), abstract 497.

Casey, B.J., Tottenham, N., Liston, C., Durston, S., 2005. Imaging the developing brain: what have we learned about cognitive development. Trends Cogn. Sci. 9 (3), 104–110, http://dx.doi.org/10.1016/j.tics.2005.01.011.

Changeux, J.P., Danchin, A., 1976. Selective stabilisation of developing synapses as a mechanism for the specification of neuronal networks. Nature 264, 705–712.

Cignetti, F., Vaugoyeau, M., Nazarian, B., Roth, M., Anton, J.L., Assaiante, C., 2014. Boosted activation of right inferior frontoparietal network: a basis for illusory movement awareness. Hum. Brain Mapp. 35 (10), 5166–5178, http://dx.doi.org/10.1002/hbm.22541.

Cignetti, F., Fontan, A., Menant, J., Nazarian, B., Anton, J.L., Vaugoyeau, M., Assaiante, C., 2016a. Protracted development of the proprioceptive brain network during and beyond adolescence. Cereb. Cortex 4, 323, http://dx.doi.org/10.1093/cercor/bhv323.

Cignetti, F., Salvia, E., Anton, J.L., Grosbras, M.H., Assaiante, C., 2016b. Pros and cons of using the informed basis set to account for hemodynamic response

variability with developmental data. Front. Neurosci. 10, 322, http://dx.doi.org/10.3389/fnins.2016.00322.
Daprati, E., Sirigu, A., Nico, D., 2010. Body and movement: consciousness in the parietal lobes. Neuropsychologia 48 (3), 756–762, http://dx.doi.org/10.1016/j.neuropsychologia.2009.10.008.
Desikan, R.S., Ségonne, F., Fischl, B., Quinn, B.T., Dickerson, B.C., Blacker, D., Buckner, R.L., Dale, A.M., Maguire, R.P., Hyman, B.T., Albert, M.S., Killiany, R.J., 2006. An automated labelling system for subdividing the human cerebral cortex on MRI scans into gyral based regions of interest. Neuroimage 1 (3), 968–980, http://dx.doi.org/10.1016/j.neuroimage.2006.01.021 (31).
Desmurget, M., Sirigu, A., 2009. A parietal-premotor network for movement intention and motor awareness. Trends Cogn. Sci. 13 (10), 411–419, http://dx.doi.org/10.1016/j.tics.2009.08.001.
Desmurget, M., Reilly, K.T., Richard, N., Szathmari, A., Mottolese, C., Sirigu, A., 2009. Movement intention after parietal cortex stimulation in humans. Science 8 (5928), 811–813, http://dx.doi.org/10.1126/science.1169896, 324.
Di Russo, F., Committeri, G., Pitzalis, S., Spitoni, G., Piccardi, L., Galati, G., Catagni, M., Nico, D., Guariglia, C., Pizzamiglio, L., 2006. Cortical plasticity following surgical extension of lower limbs. Neuroimage 30 (1), 172–183, http://dx.doi.org/10.1016/j.neuroimage.2005.09.051.
Durston, S., Davidson, M.C., Tottenham, N., Galvan, A., Spicer, J., Fossella, J.A., Casey, B.J., 2006. A shift from diffuse to focal cortical activity with development. Dev. Sci. 9 (1), 1–8, http://dx.doi.org/10.1111/j.1467-7687.2005.00454.x.
Ehrsson, H.H., Geyer, S., Naito, E., 2003. Imagery of voluntary movement of fingers, toes, and tongue activates corresponding Body-part-specific motor representations. J. Neurophysiol. 90, 3304–3316, http://dx.doi.org/10.1152/jn.01113.2002.
Ehrsson, H.H., Kito, T., Sadato, N., Passingham, R.E., Naito, E., 2005. Neural substrate of body size: illusory feeling of shrinking of the waist. PLoS Biol. 3 (12), e412, http://dx.doi.org/10.1371/journal.pbio.0030412.
Fair, D.A., Dosenbach, N.U., Church, J.A., Cohen, A.L., Brahmbhatt, S., Miezin, F.M., Barch, D.M., Raichle, M.E., Petersen, S.E., Schlaggar, B.L., 2007. Development of distinct control networks through segregation and integration. Proc. Natl. Acad. Sci. U. S. A. 14 (33), 13507–13512, http://dx.doi.org/10.1073/pnas.0705843104 (104).
Fair, D.A., Nigg, J.T., Iyer, S., Bathula, D., Mills, K.L., Dosenbach, N.U., Schlaggar, B.L., Mennes, M., Gutman, D., Bangaru, S., Buitelaar, J.K., Dickstein, D.P., Di Martino, A., Kennedy, D.N., Kelly, C., Luna, B., Schweitzer, J.B., Velanova, K., Wang, Y.F., Mostofsky, S., Castellanos, F.X., Milham, M.P., 2013. Distinct neural signatures detected for ADHD subtypes after controlling for micro-movements in resting state functional connectivity MRI data. Front. Syst. Neurosci. 4 (6), 80, http://dx.doi.org/10.3389/fnsys.2012.00080.
Formisano, E., Di Salle, F., Goebel, R., 2005. Fundamentals of data analysis methods in functional MRI. In: Landini, L., Positano, V., Santarelli, M.F. (Eds.), Advanced Imaging Processing in Magnetic Resonance Imaging. CRC Taylor, Francis, pp. 481–503.
Friston, K.J., Holmes, A.P., Poline, J.B., Grasby, P.J., Williams, S.C., Frackowiak, R.S., Turner, R., 1995. Analysis of fMRI time-series revisited. Neuroimage 2, 45–53, http://dx.doi.org/10.1006/nimg.1995.1007.
Friston, K.J., Williams, S., Howard, R., Frackowiak, R.S., Turner, R., 1996. Movement-related effects in fMRI time-series. Magn. Reson. Med. 35 (3), 346–355.
Gao, W., Alcauter, S., Smith, J.K., Gilmore, J.H., Lin, W., 2015. Development of human brain cortical network architecture during infancy. Brain Struct. Funct. 220 (2), 1173–1186, http://dx.doi.org/10.1007/s00429-014-0710-3.
Gazzaley, A., D'Esposito, M., 2007. Top-Down modulation and normal aging. Ann. N. Y. Acad. Sci. 1097, 67–83, http://dx.doi.org/10.1196/annals.1379.010.
Gazzaley, A., Rissman, J., Cooney, J., Rutman, A., Seibert, T., Clapp, W., D'Esposito, M., 2007. Functional interactions between prefrontal and visual association cortex contribute to top-down modulation of visual processing. Cereb. Cortex 17 (Suppl. 1), i125–35, http://dx.doi.org/10.1093/cercor/bhm113.
Goble, D.J., Lewis, C.A., Hurvitz, E.A., Brown, S.H., 2005. Development of upper limb proprioceptive accuracy in children and adolescents. Hum. Mov. Sci. 24 (2), 155–170, http://dx.doi.org/10.1016/j.humov.2005.05.004.
Goble, D.J., Coxon, J.P., Van Impe, A., Geurts, M., Van Hecke Sunaert, S., Wenderoth, N., Swinnen, S.P., 2012. The neural basis of central proprioceptive processing in older versus younger adults: an important sensory role for right putamen. Hum. Brain Mapp. 33, 895–908.
Goble, D.J., 2010. Proprioceptive acuity assessment via joint position matching: from basic science to general practice. Phys. Ther. 90 (8), 1176–1184, http://dx.doi.org/10.2522/ptj.20090399.
Gogtay, N., Giedd, J.N., Lusk, L., Hayashi, K.M., Greenstein, D., Vaituzis, A.C., Nugent 3rd, T.F., Herman, D.H., Clasen, L.S., Toga, A.W., Rapoport, J.L., Thompson, P.M., 2004. Dynamic mapping of human cortical development during childhood through early adulthood. Proc. Natl. Acad. Sci. U. S. A. 25, http://dx.doi.org/10.1073/pnas.0402680101.
Good, C.D., Johnsrude, I.S., Ashburner, J., Henson, R.N., Friston, K.J., Frackowiak, R.S., 2001. A voxel-based morphometric study of ageing in 465 normal adult human brains. Neuroimage 14 (1 Pt 1), 21–36, http://dx.doi.org/10.1006/nimg.2001.0786.
Hagura, N., Oouchida, Y., Aramaki, Y., Okada, T., Matsumura, M., Sadato, N., Naito, E., 2009. Visuokinesthetic perception of hand movement is mediated by cerebro-cerebellar interaction between the left cerebellum and right parietal cortex. Cereb. Cortex 19 (1), 176–186, http://dx.doi.org/10.1093/cercor/bhn068.
Hilgenstock, R., Weiss, T., Witte, O.W., 2014. You'd better think twice: post-decision perceptual confidence. Neuroimage 1 (October (99)), 323–331, http://dx.doi.org/10.1016/j.neuroimage.2014.05.049.
Holmes, A., Friston, K.J., 1998. Generalisability, random effects and population inference. Neuroimage 7, S754.
Innocenti, G.M., Price, D.J., 2005. Exuberance in the development of cortical networks. Nat. Rev. Neurosci. 6, 955–965, http://dx.doi.org/10.1038/nrn1790.
Jenkinson, M., Bannister, P., Brady, J.M., Smith, S.M., 2002. Improved optimisation for the robust and accurate linear registration and motion correction of brain images. Neuroimage 17 (2), 825–841.
Jolles, D.D., van Buchem, M.A., Crone, E.A., Rombouts, S.A., 2011. A comprehensive study of whole-brain functional connectivity in children and young adults. Cereb. Cortex 21 (2), 385–391, http://dx.doi.org/10.1093/cercor/bhq104.
Kelly, A.M., Di Martino, A., Uddin, L.Q., Shehzad, Z., Gee, D.G., Reiss, P.T., Margulies, D.S., Castellanos, F.X., Milham, M.P., 2009. Development of anterior cingulate functional connectivity from late childhood to early adulthood. Cereb. Cortex 19, 640–657, http://dx.doi.org/10.1093/cercor/bhn117.
Koechlin, E., Hyafil, A., 2007. Anterior prefrontal function and the limits of human decision-making. Science 5850, 594–598, http://dx.doi.org/10.1126/science.1142995 (Review).
Koechlin, E., Danek, A., Burnod, Y., Grafman, J., 2002. Medial prefrontal and subcortical mechanisms underlying the acquisition of motor and cognitive action sequences in humans. Neuron 18, 371–381.
Lebel, C., Beaulieu, C., 2011. Longitudinal development of human brain wiring continues from childhood into adulthood. J. Neurosci. 27 (30), 10937–10947, http://dx.doi.org/10.1523/JNEUROSCI.5302-10.2011 (31).
Lebel, C., Walker, L., Leemans, A., Phillips, L., Beaulieu, C., 2008. Microstructural maturation of the human brain from childhood to adulthood. Neuroimage 15 (3), 1044–1055, http://dx.doi.org/10.1016/j.neuroimage.2007.12.053 (40).
Lebel, C., Gee, M., Camicioli, R., Wieler, M., Martin, W., Beaulieu, C., 2012. Diffusion tensor imaging of white matter tract evolution over the lifespan. Neuroimage 60 (1), 340–352, http://dx.doi.org/10.1016/j.neuroimage.2011.11.094.
Longo, M.R., Haggard, P., 2010. An implicit body representation underlying human position sense. Proc. Natl. Acad. Sci. U. S. A. 107 (26), 11727–11732, http://dx.doi.org/10.1073/pnas.1003483107.
Lu, L.H., Dapretto, M., O'Hare, E.D., Kan, E., McCourt, S.T., Thompson, P.M., Toga, A.W., Bookheimer, S.Y., Sowell, E.R., 2009. Relationships between brain activation and brain structure in normally developing children. Cereb. Cortex 19 (11), 2595–2604, http://dx.doi.org/10.1093/cercor/bhp011.
Ludwig, V.U., Seitz, J., Schönfeldt-Lecuona, C., Höse, A., Abler, B., Hole, G., Goebel, R., Walter, H., 2015. The neural correlates of movement intentions: a pilot study comparing hypnotic and simulated paralysis. Conscious Cogn. Sep; 35, 158–170, http://dx.doi.org/10.1016/j.concog.2015.05.010.
Luna, B., Padmanabhan, A., O'Hearn, K., 2010. What has fMRI told us about the development of cognitive control through adolescence. Brain Cogn. 72 (1), 101–113, http://dx.doi.org/10.1016/j.bandc.2009.08.005.
Makris, N., Goldstein, J.M., Kennedy, D., Hodge, S.M., Caviness, V.S., Faraone, S.V., Tsuang, M.T., Seidman, L.J., 2006. Decreased volume of left and total anterior insula lobule in schizophrenia. Schizophr. Res. 83 (2-3), 155–157, http://dx.doi.org/10.1016/j.schres.2005.11.020.
Mars, R.B., Coles, M.G., Hulstijn, W., Toni, I., 2008. Delay-related cerebral activity and motor preparation. Cortex 44 (5), 507–520.
Miller, E.K., Cohen, J.D., 2001. An integrative theory of prefrontal cortex function. Annu. Rev. Neurosci. 24, 167–202, http://dx.doi.org/10.1146/annurev.neuro.24.1.167.
Mori, S., Oishi, K., Jiang, H., Jiang, L., Li, X., Akhter, K., Hua, K., Faria, A.V., Mahmood, A., Woods, R., Toga, A.W., Pike, G.B., Neto, P.R., Evans, A., Zhang, J., Huang, H., Miller, M.I., van Zijl, P., Mazziotta, J., 2008. Stereotaxic white matter atlas based on diffusion tensor imaging in an ICBM template. Neuroimage 1, 2007, http://dx.doi.org/10.1016/j.neuroimage.2007.12.035.
Naito, E., Ehrsson, H.H., 2006. Somatic sensation of hand-object interactive movement is associated with activity in the left inferior parietal cortex. J. Neurosci. 5 (14), 3783–3790, http://dx.doi.org/10.1523/JNEUROSCI.4835-05.2006 (26).
Naito, E., Ehrsson, H.H., Geyer, S., Zilles, K., Roland, P.E.J., 1999. Illusory arm movements activate cortical motor areas: a positron emission tomography study. Neurosci 15, 6134–6144.
Naito, E., Roland, P.E., Ehrsson, H.H., 2002. I feel my hand moving: a new role of the primary motor cortex in somatic perception of limb movement. Neuron 5, 979–988.
Naito, E., Roland, P.E., Grefkes, C., Choi, H.J., Eickhoff, S., Geyer, S., Zilles, K., Ehrsson, H.H., 2005. Dominance of the right hemisphere and role of area 2 in human kinesthesia. J. Neurophysiol. 93, 1020–1034, http://dx.doi.org/10.1152/jn.00637.2004.
Naito, E., Morita, T., Amemiya, K., 2016. Body representations in the human brain revealed by kinesthetic illusions and their essential contributions to motor control and corporeal awareness. Neurosci. Res. 104, 16–30, http://dx.doi.org/10.1016/j.neures.2015.10.013.
Paus, T., 2010. Growth of white matter in the adolescent brain: myelin or axon. Brain Cogn. 72 (1), 26–35, http://dx.doi.org/10.1016/j.bandc.2009.06.002.
Power, J.D., Barnes, K.A., Snyder, A.Z., Schlaggar, B.L., Petersen, S.E., 2012. Spurious but systematic correlations in functional connectivity MRI networks arise from subject motion. Neuroimage 1 (3), 2142–2154, http://dx.doi.org/10.1016/j.neuroimage.2011.10.018 (59).

Proske, U., Gandevia, S.C., 2012. The proprioceptive senses: their roles in signaling body shape, body position and movement, and muscle force. Physiol. Rev. 92 (4), 1651–1697, http://dx.doi.org/10.1152/physrev.00048.2011.
Qin, S., Young, C.B., Supekar, K., Uddin, L.Q., Menon, V., 2012. Immature integration and segregation of emotion-related brain circuitry in young children. Proc. Natl. Acad. Sci. U. S. A. 109 (May (20)), 7941–7946, http://dx.doi.org/10.1073/pnas.1120408109 (15).
Radovanovic, S., Korotkov, A., Ljubisavljevic, M., Lyskov, E., Thunberg, J., Kataeva, G., Danko, S., Roudas, M., Pakhomov, S., Medvedev, S., Johansson, H., 2002. Comparison of brain activity during different types of proprioceptive inputs: a positron emission tomography study. Exp. Brain Res. 143 (3), 276–285.
Rakic, P., Bourgeois, J.P., Goldman-Rakic, P.S., 1994. Synaptic development of the cerebral cortex: implications for learning, memory, and mental illness. Prog. Brain Res. 102, 227–243, http://dx.doi.org/10.1016/S0079-6123(08)60543-9.
Rakic, P., Ayoub, A.E., Breunig, J.J., Dominguez, M.H., 2009. Decision by division: making cortical maps. Trends Neurosci. 32, 291–301, http://dx.doi.org/10.1016/j.tins.2009.01.007.
Raos, V., Savaki, H.E., 2016. The role of the prefrontal cortex in action perception. Cereb. Cortex, http://dx.doi.org/10.1093/cercor/bhw261.
Roll, J.P., Vedel, J.P., 1982. Kinaesthetic role of muscle afferents in man, studied by tendon vibration and microneurography. Exp. Brain Res. 47 (2), 177–190.
Roll, J.P., Vedel, J.P., Ribot, E., 1989. Alteration of proprioceptive messages induced by tendon vibration in man: a microneurographic study. Exp. Brain Res. 76 (1), 213–222.
Rushworth, M.F., Johansen-Berg, H., Gobel, S.M., Devlin, J.T., 2003. The left parietal and premotor cortices: motor attention and selection. Neuroimage 1, S89–100.
Shaw, P., Kabani, N.J., Lerch, J.P., Eckstrand, K., Lenroot, R., Gogtay, N., Greenstein, D., Clasen, L., Evans, A., Rapoport, J.L., Giedd, J.N., Wise, S.P., 2008. Neurodevelopmental trajectories of the human cerebral cortex. J. Neurosci. 2 (14), 3586–3594, http://dx.doi.org/10.1523/JNEUROSCI.5309-07.2008 (28).
Simmonds, D.J., Hallquist, M.N., Asato, M., Luna, B., 2014. Developmental stages and sex differences of white matter and behavioral development through adolescence: a longitudinal diffusion tensor imaging (DTI) study. Neuroimage 15 (92), 356–368, http://dx.doi.org/10.1016/j.neuroimage.2013.12.044.
Smith, S.M., Jenkinson, M., Woolrich, M.W., Beckmann, C.F., Behrens, T.E.J., Johansen-Berg, H., Bannister, P.R., De Luca, M., Drobnjak, I., Flitney, D.E., Niazy, R., Saunders, J., Vickers, J., Zhang, Y., De Stefano, N., Brady, J.M., Matthews, P.M., 2004. Advances in functional and structural MR image analysis and implementation as FSL. Neuroimage 23 (S1), 208–219, http://dx.doi.org/10.1016/j.neuroimage.2004.07.051.
Smith, S.M., 2002. Fast robust automated brain extraction. Hum. Brain Mapp. 17 (3), 143–155, http://dx.doi.org/10.1002/hbm.10062.
Sowell, E.R., Thompson, P.M., Holmes, C.J., Batth, R., Jernigan, T.L., Toga, A.W., 1999. Localizing age-related changes in brain structure between childhood and adolescence using statistical parametric mapping. Neuroimage 9 (6 Pt 1), 587–597, http://dx.doi.org/10.1006/nimg.1999.0436.
Tamm, L., Menon, V., Reiss, A.L., 2002. Maturation of brain function associated with response inhibition. J. Am. Acad. Child Adolesc. Psychiatry 41 (10), 1231–1238, http://dx.doi.org/10.1097/00004583-200210000-00013.
Toni, I., Schluter, N.D., Josephs, O., Friston, K., Passingham, R.E., 1999. Signal-, set- and movement-related activity in the human brain: an event related fMRI study. Cereb. Cortex 9, 35–49.
Wakana, S., Caprihan, A., Panzenboeck, M.M., Fallon, J.H., Perry, M., Gollub, R.L., Hua, K., Zhang, J., Jiang, H., Dubey, P., Blitz, A., van Zijl, P., Mori, S., 2007. Reproducibility of quantitative tractography methods applied to cerebral white matter. Neuroimage 1 (3), 630–644, http://dx.doi.org/10.1016/j.neuroimage.2007.02.049 (36).
Wendelken, C., O'Hare, E.D., Whitaker, K.J., Ferrer, E., Bunge, S.A., 2011. Increased functional selectivity over development in rostrolateral Prefrontal Cortex. J. Neurosci. 23 (47), 17260–17268, http://dx.doi.org/10.1523/jneurosci.1193-10.2011 (31).
Woo, C.W., Krishnan, A., Wager, T.D., 2014. Cluster-extent based thresholding in fMRI analyses: pitfalls and recommendations. Neuroimage 1 (91), 412–419, http://dx.doi.org/10.1016/j.neuroimage.2013.12.058.
Yan, C.G., Cheung, B., Kelly, C., Colcombe, S., Craddock, R.C., Di Martino, A., Li, Q., Zuo, X.N., Castellanos, F.X., Milham, M.P., 2013. A comprehensive assessment of regional variation in the impact of head micromovements on functional connectomics. Neuroimage 1 (76), 183–201, http://dx.doi.org/10.1016/j.neuroimage.2013.03.004.
Yendiki, A., Koldewyn, K., Kakunoori, S., Kanwisher, N., Fischl, B., 2014. Spurious group differences due to head motion in a diffusion MRI study. Neuroimage 88, 79–90, http://dx.doi.org/10.1016/j.neuroimage.2013.11.027.
Zielinski, B.A., Gennatas, E.D., Zhou, J., Seeley, W.W., 2010. Network-level structural covariance in the developing brain. Proc. Natl. Acad. Sci. USA. 19, http://dx.doi.org/10.1073/pnas.1003109107.